Basics and applications of photothermal beam deflection spectroscopy

Dorota Korte
Laboratory for Environmental Research,
University of Nova Gorica, Slovenia

Photothermal defelction (mirage-effect) spectroscopy

a non-destructive and highly-sensitive technique

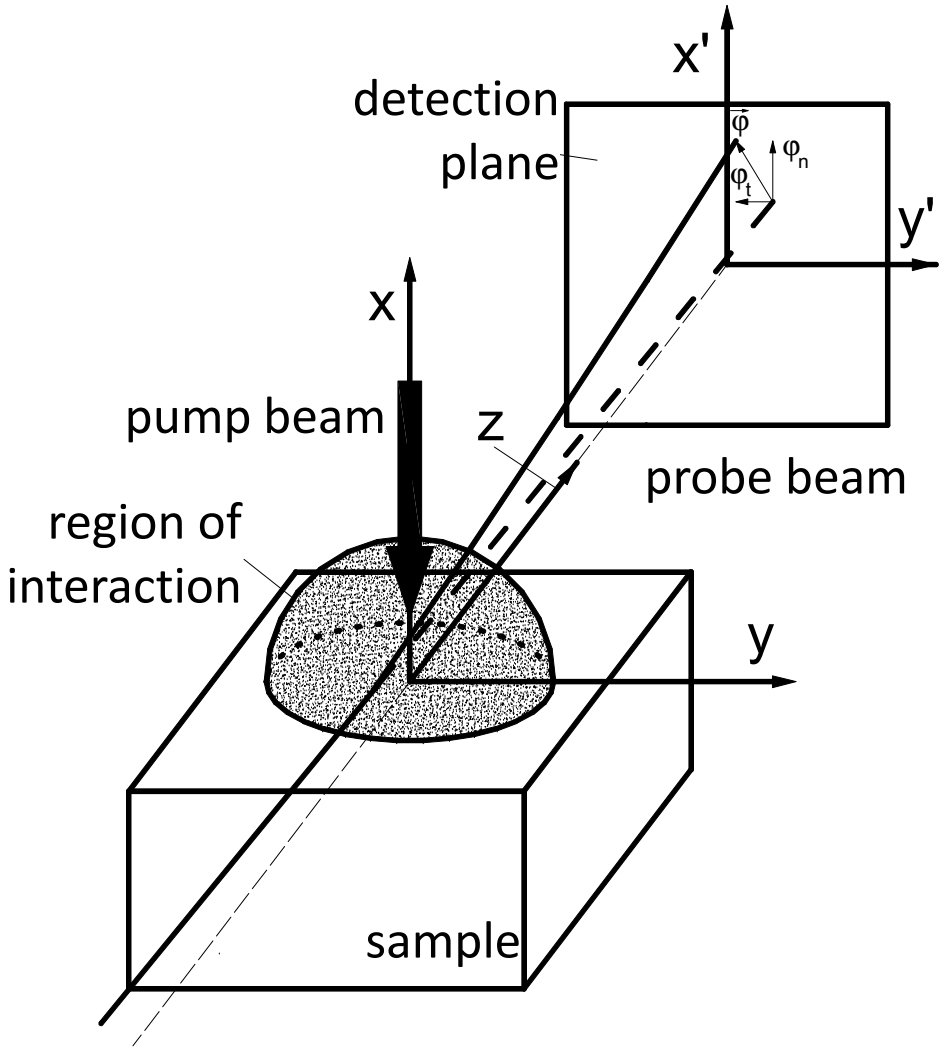

φ_n, φ_t – normal and tangrntinal deflection of the probe beam;

- Spectroscopy measures the light absorption in order to quatitatively identify substances of interest
- The photothermal effect heats a sample upon absorption of electromagnetic radiation
- Refractive index change from photothermal temperature change produces an optical signal
- To increase the sensitivity of this technique, the sample is generally placed in a cell containing a transparent liquid, the refractive index of which depends strongly on temperature

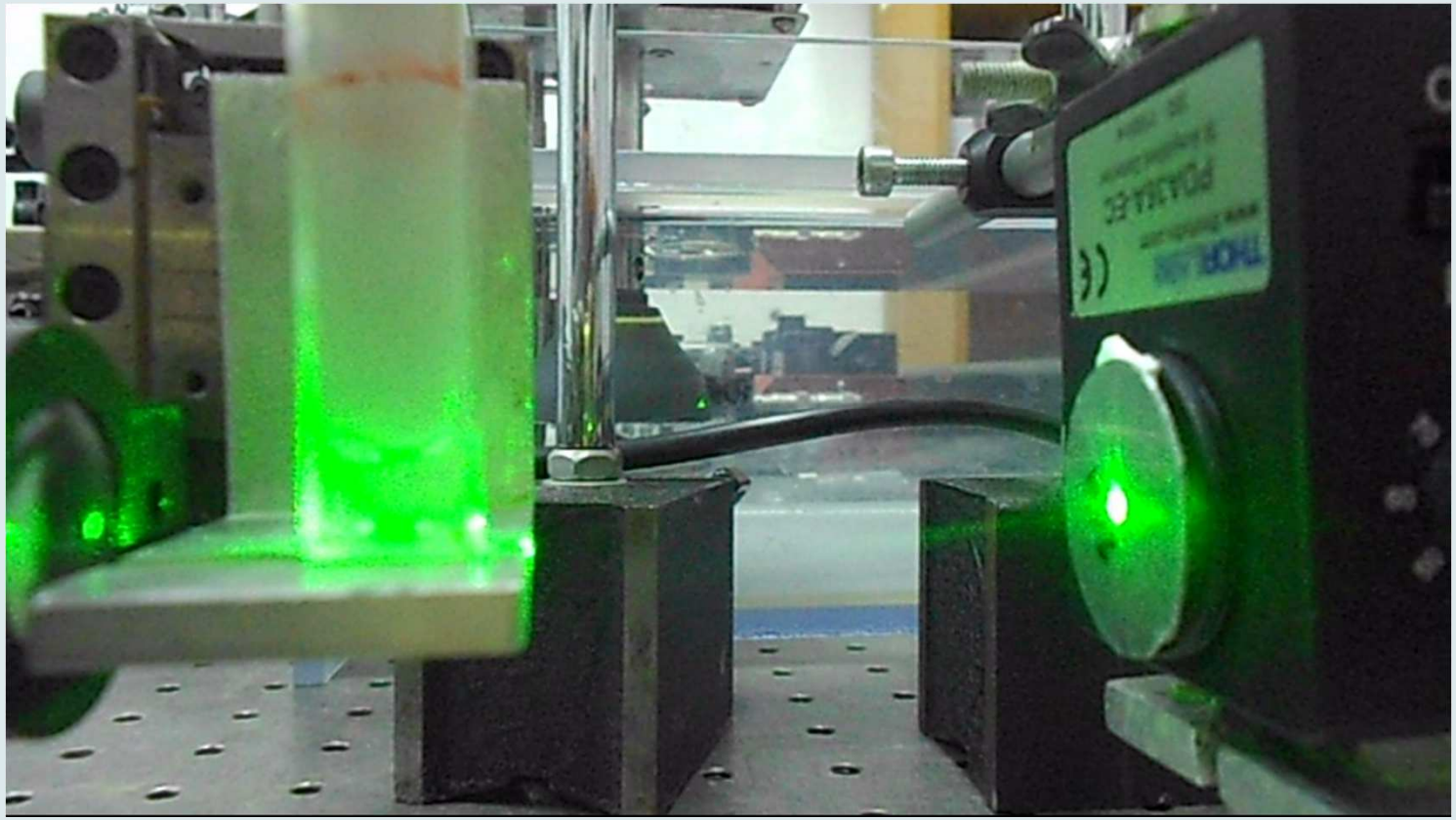
THOR LABS
POLARIZER

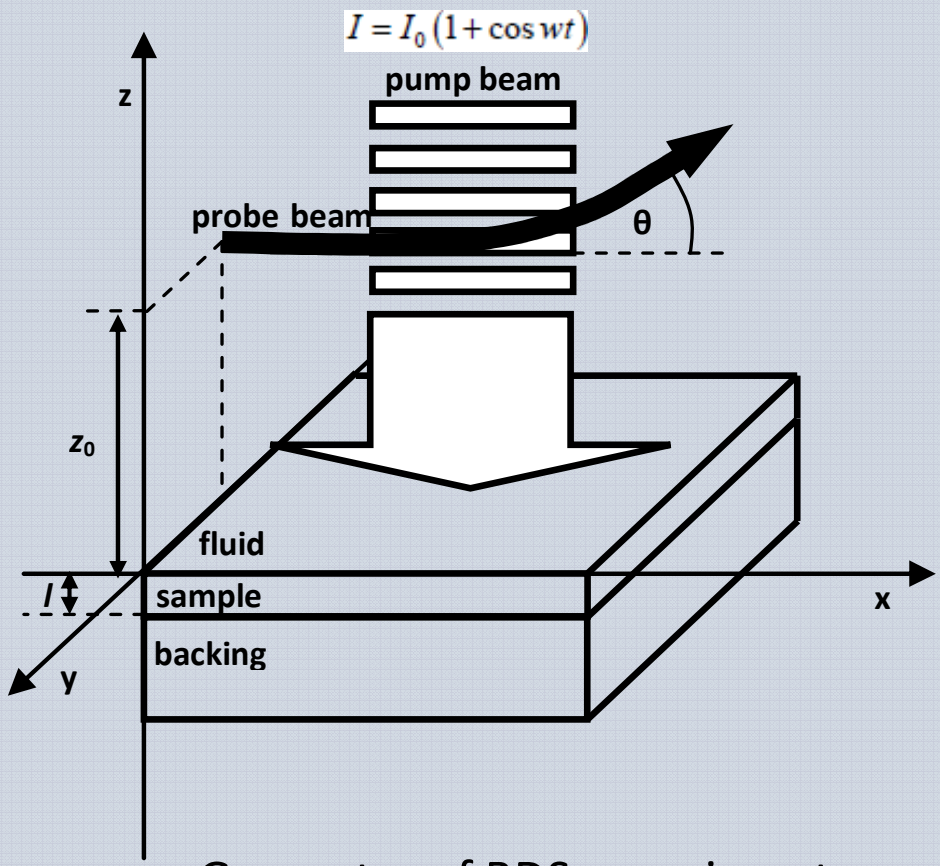

Geometry of BDS experiments

Thermal conductivity describes the material's ability to conduct heat.

Thermal diffusivity measures the ability of a material to conduct thermal energy relative to its ability to store it.

Heat diffusion (Fourier-Kirchhof) equation:

$$\frac{1}{\kappa}\frac{\partial\theta}{\partial t} = \frac{\partial^2\theta}{\partial z^2} + \frac{q}{k}$$

κ - thermal diffusivity, m^2s^{-1}

k - thermal conductivity, $Wm^{-1}K^{-1}$

q - volume denisity of heat sources, Wm^{-3}

θ - temperature distribution,

t - time

Boundary condition:

- equality of the temperature distribution

$$\theta_1 = \theta_2 \;,\; \theta_2 = \theta_3 \quad \text{etc.}$$

- equality of the heat flow

$$j_1 = j_2 \;,\; j_2 = j_3 \quad \text{etc.}$$

at the fluid-sample-fluid (backing) boundaries.

Fourier law:

$$j = k\frac{\partial\theta}{\partial z}$$

Thermal waves

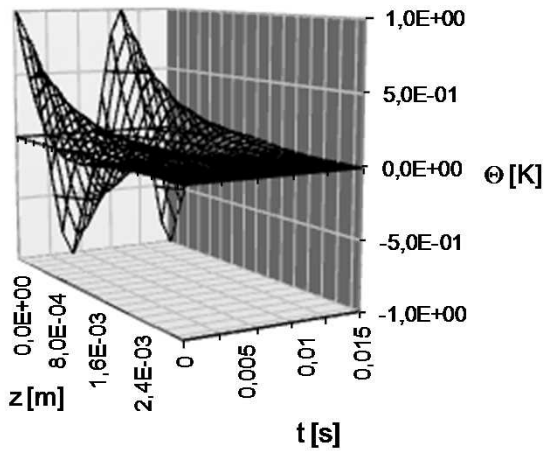

$$\Theta(z,t) = \Theta_m \exp\left(-\sqrt{\frac{\Omega}{2\kappa}}z\right)\cos\left(\Omega t - \sqrt{\frac{\Omega}{2\kappa}}z + \varphi\right)$$

damping factor (attenuation=wave number):

$$k_{th} = \sqrt{\frac{\Omega}{2\kappa}}$$

Ω-modulation frequency of temperature field

Thermal diffusion length: $\mu_{th} = \dfrac{1}{k_{th}}$ $\kappa = k/\rho c$, ρ - denisity, c - specific heat

The thermal waves change the fluid refractive index:

$$n(T) \cong n_0 + \left.\frac{dn}{dT}\right|_{T_0}(T - T_0) = n_0 + n_0 s_T \theta_g(z,t)$$

n_0 - the index of refraction in ambient temperature T_0, s_T is the refractive index thermal sensitivity.

Typical geometries of measuring setup for detection using mirage effect

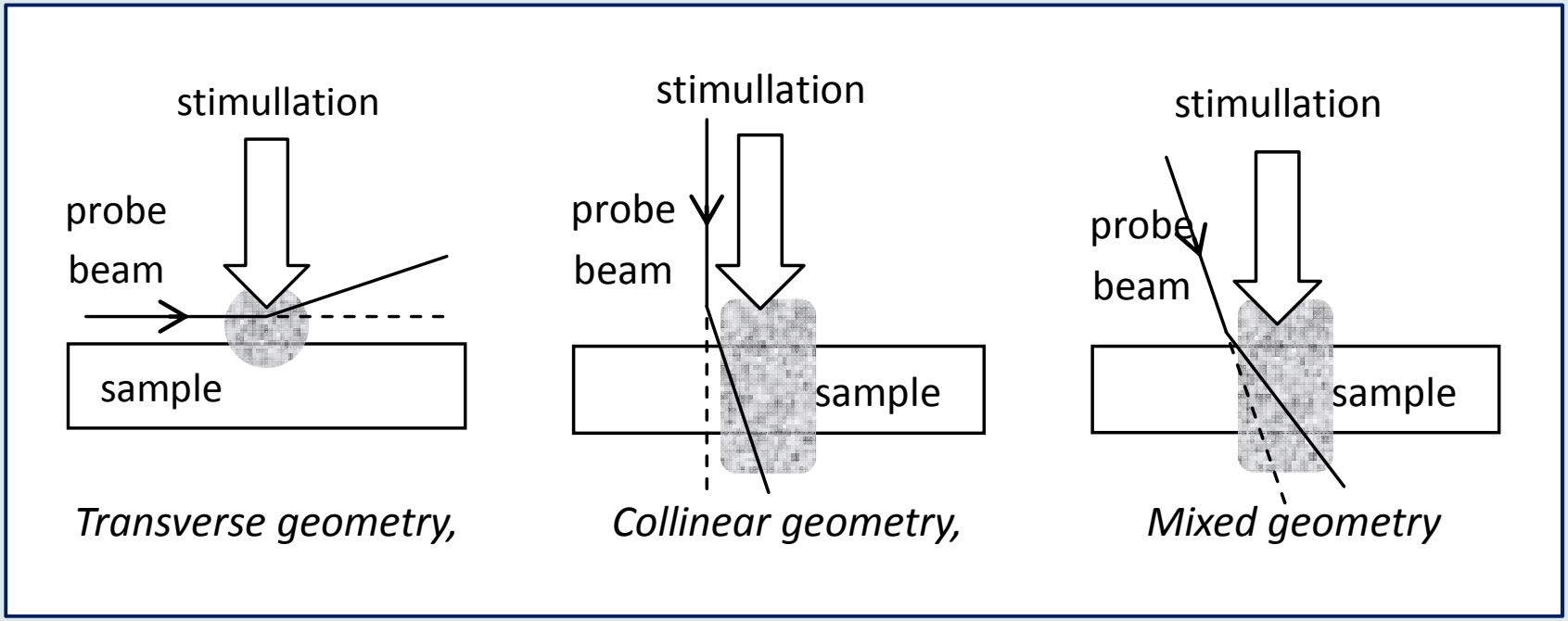

Theoretical discription

THE RAY DEFLECTION THEORY

The angle of normal deflection of the single ray propagating through the ThWs:

$$\phi_n = -\left(\frac{1}{n}\frac{dn}{dT}\right)\Bigg|_{T_0} \int_{z_l}^{z_p} \frac{\partial \theta_g(x,t)}{\partial x} dz$$

THE RAY DEFLECTION AVERAGING THEORY (RDAT)

$$\psi_n = \int_{x=-h}^{+\infty} \int_{-\infty}^{+\infty} N(x,y)\phi_n(x,y)dxdy \qquad N(x,y) = \frac{\exp\left[-\frac{(x-x_0)^2+(y-y_0)^2}{a^2}\right]}{\int_{x=-h}^{+\infty}\int_{y=-\infty}^{+\infty} \exp\left[-\frac{(x-x_0)^2+(y-y_0)^2}{a^2}\right]dxdy}$$

Temperature gradient → gradient of the refractive index (thermal lens) → deflection of the light ray

THE WAVE THEORY (WT)

The change of the distribution of the electric field in the probe beam due to its interaction with the temperature field:

$$\Delta u(x, y, z) \approx i\Delta\phi u_0(x, y, z)$$

$u_0(x, y, z)$ the distribution of the field in the absence of the thermal lens.
The change of the phase $\Delta\phi$ due to passing through the temperature field is described by the formula:

$$\Delta\phi = \frac{2\pi}{\lambda}\frac{dn}{dT}\bigg|_{T_0}\int_{z_l}^{z_p}\theta_g(x,t)dz$$

temperature field → change in the phase of electric field → change in the intensity distribution of the probe beam

Distortions of amplitude distribution caused by deflection on refractive index gradients are not considered.

THE COMPLEX RAY THEORY (CRT)

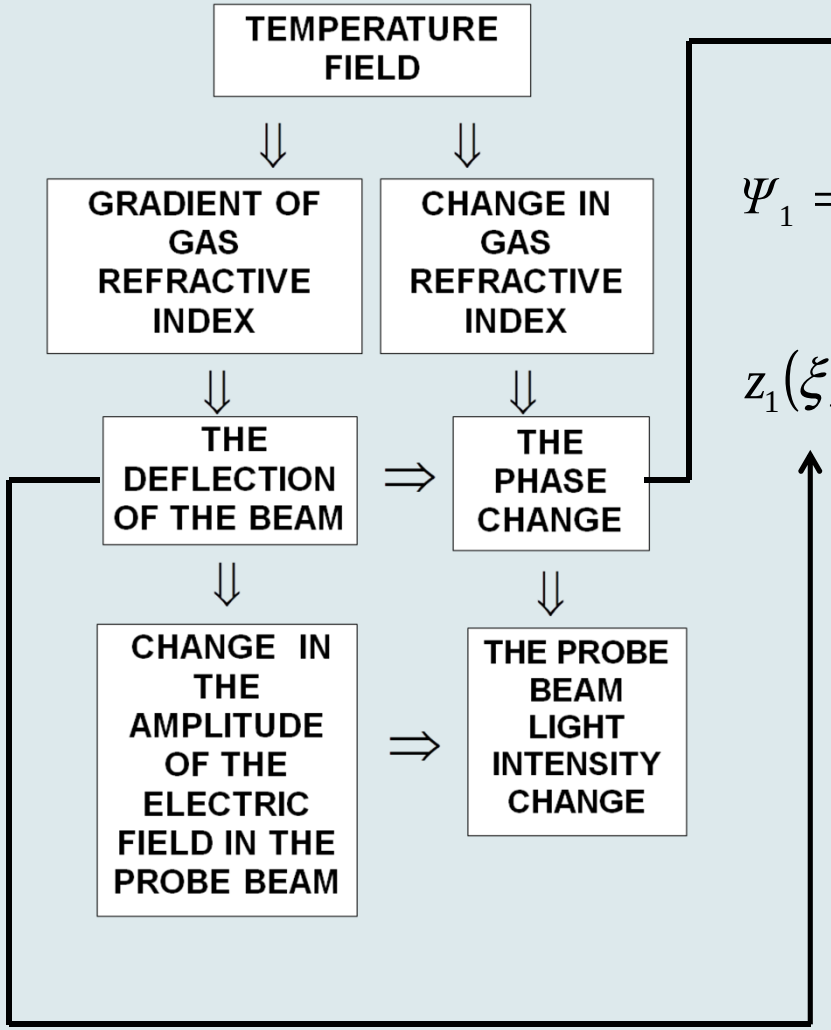

$$\Psi_1 = kn_0^2 s_T \int_0^{\tau} \vartheta_f \left[z(\tau')\right] d\tau' = \Psi_{1d} + \Psi_{1f}.$$

$$z_1(\xi,\tau) = n_0^2 s_T \int_0^{\tau} (\tau - \tau') \frac{\partial \vartheta_f}{\partial z} d\tau'$$

The phase change is caused by:

- **the change of the optical path of the ray after undergoing the thermal lens (because of the refraction index value change),**
- **the change of the geometrical path of the ray (because of the refraction index gradient).**

The deflection results from the gradient of the refractive index and causes the ray trajectory change in the temperature field.

Gaussian beam

a – probe beam radius in the waist, L – waist position, z_R –Rayleigh's length, f_L focal lengh, , $k = 2\pi/\lambda_0$, λ_0 wave length in vacuum

$$a = a_0 \frac{\frac{f_L}{z_{R0}}}{\sqrt{1+\left(\frac{f_L}{z_{R0}}\right)^2}} \qquad L = \frac{f_L}{1+\left(\frac{f_L}{z_{R0}}\right)^2}$$

$$a(z) = a\sqrt{1+\frac{(z-L)^2}{z_R^2}}$$

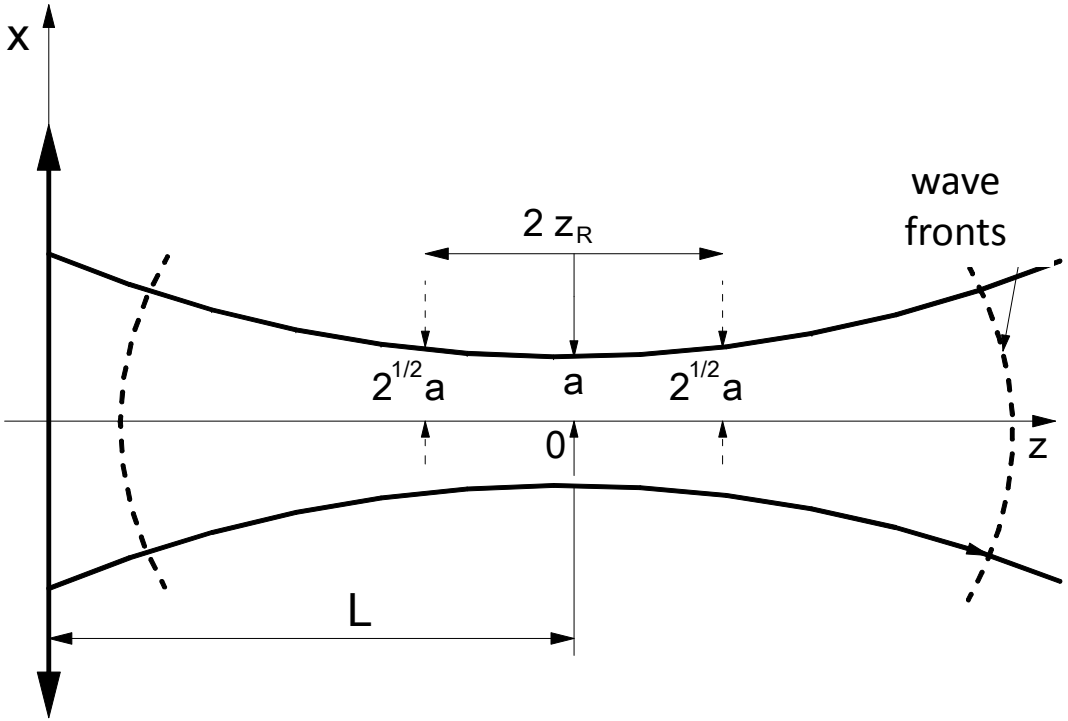

Gaussian beam is a beam of monochromatic EM radiation whose transverse magnetic and electric field amplitude profiles are given by the Gaussian function; this also implies a Gaussian intensity profile

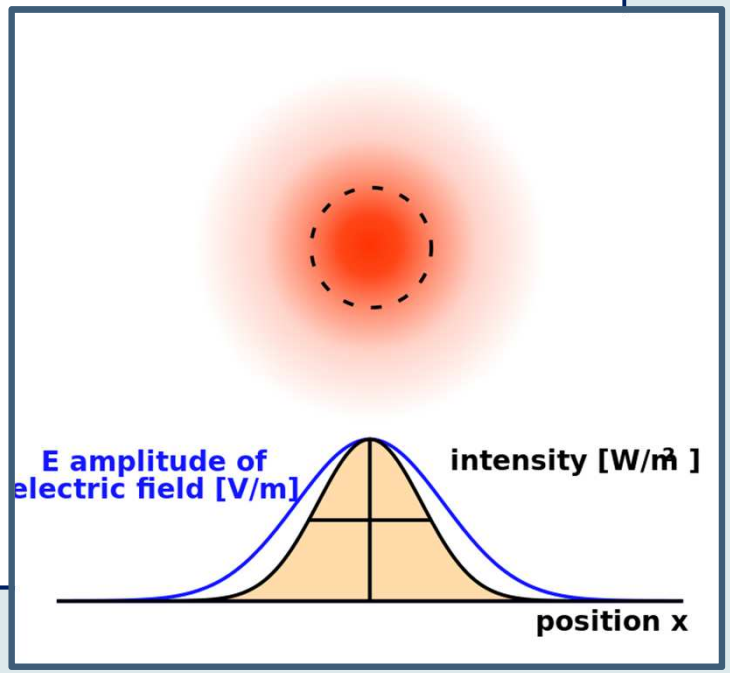

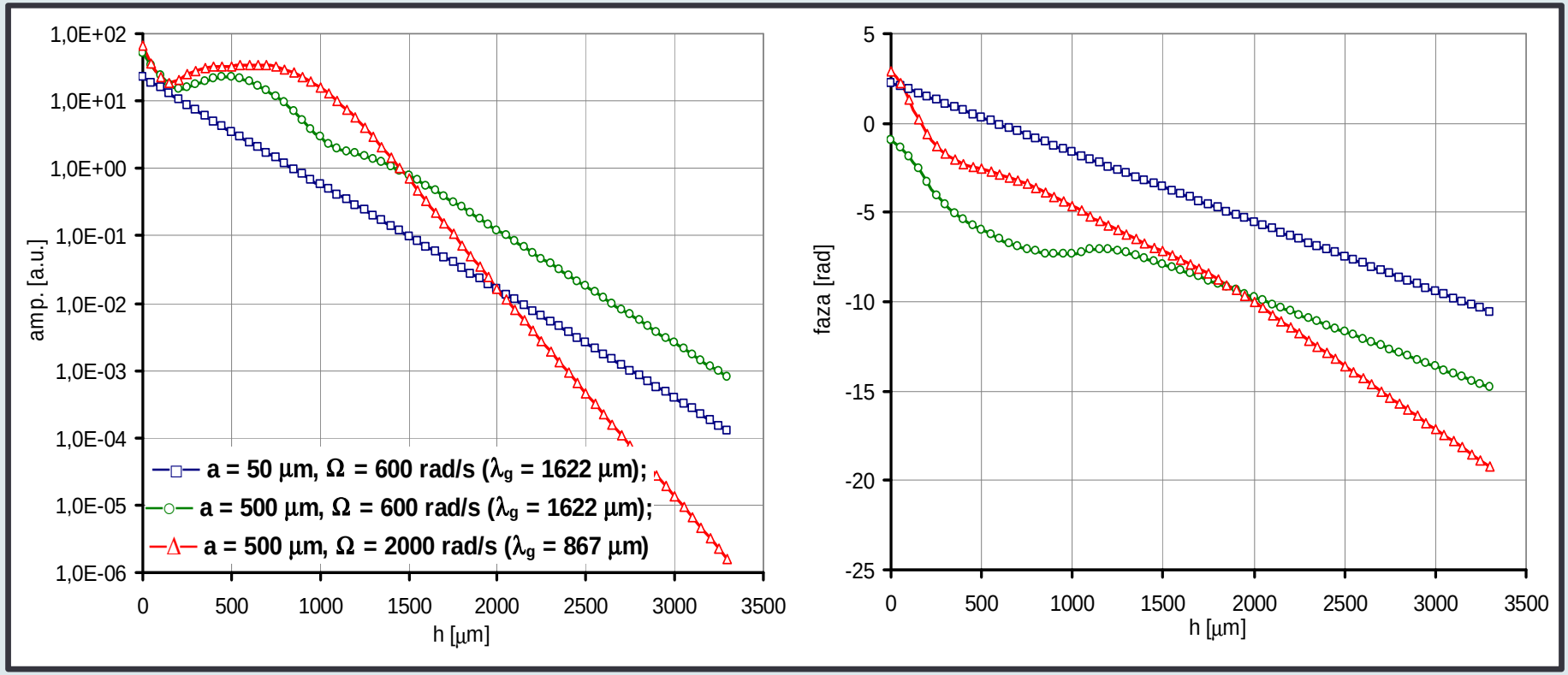

Ω – change the angle of inclination of amplitude and phase of BDS signal,
a – influence on the signal value and the character of the curves

With the increase in height of PB over the sample's surface the signal decreases since the ThWs are strongly damped in the medium.

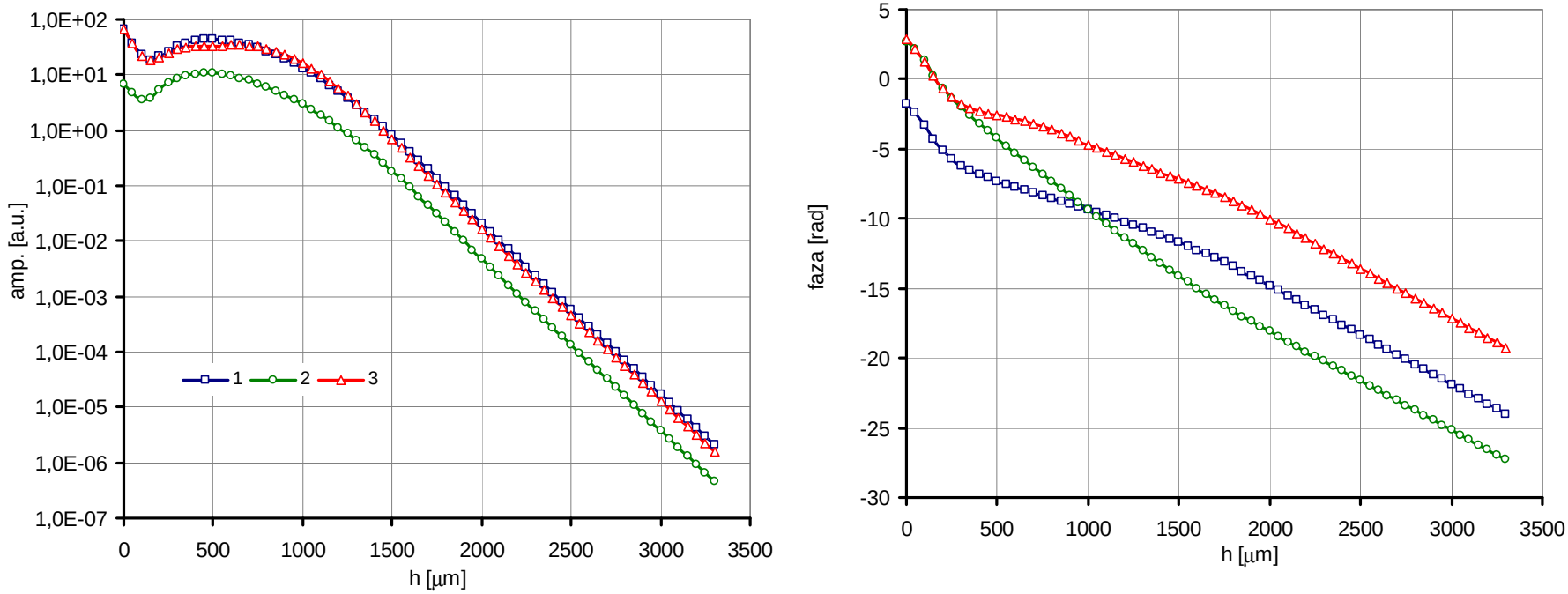

1–deflecion, 2 –phase change, 3 – total

For wide PB (*a* ~ length of ThW in air) :

⇒ deflectional component of the signal dominates.

⇒ PB is only partially disturbed by ThW

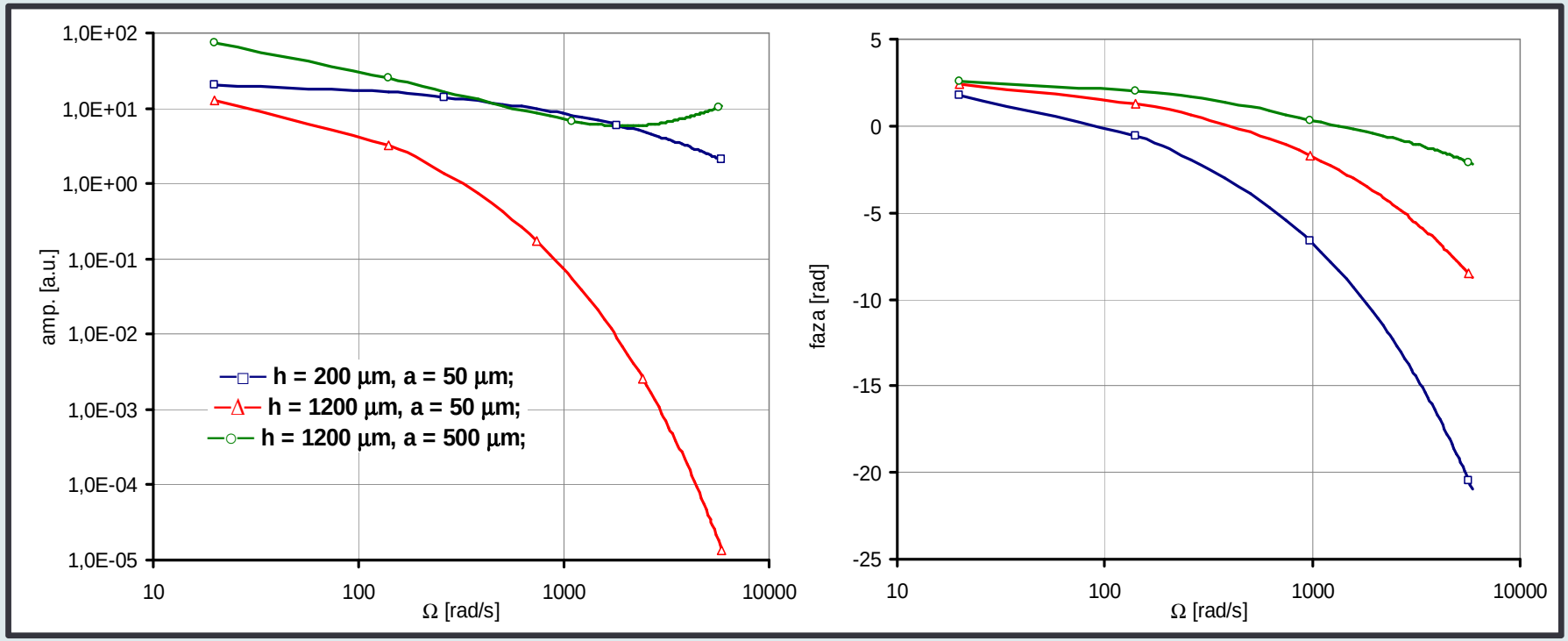

With the increase in modulation frequency of pump beam the attenuation of ThWs increases and thus the signal decreases.

With the increase in modulation frequency of pump beam the temperature gradient increases, what causes the increase of deflectional component of the signal. In cases when it dominates, the total signal increases.

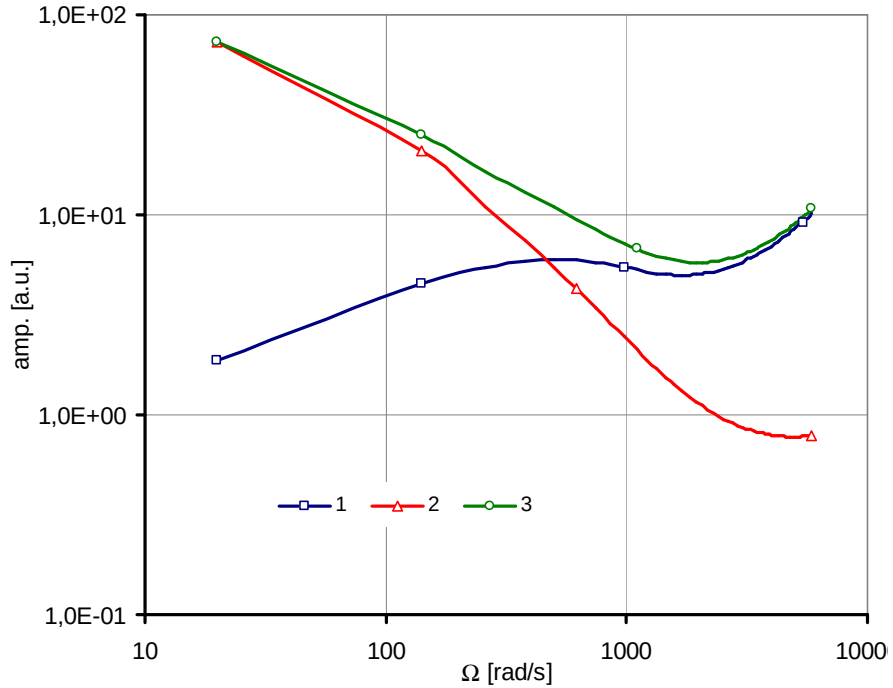

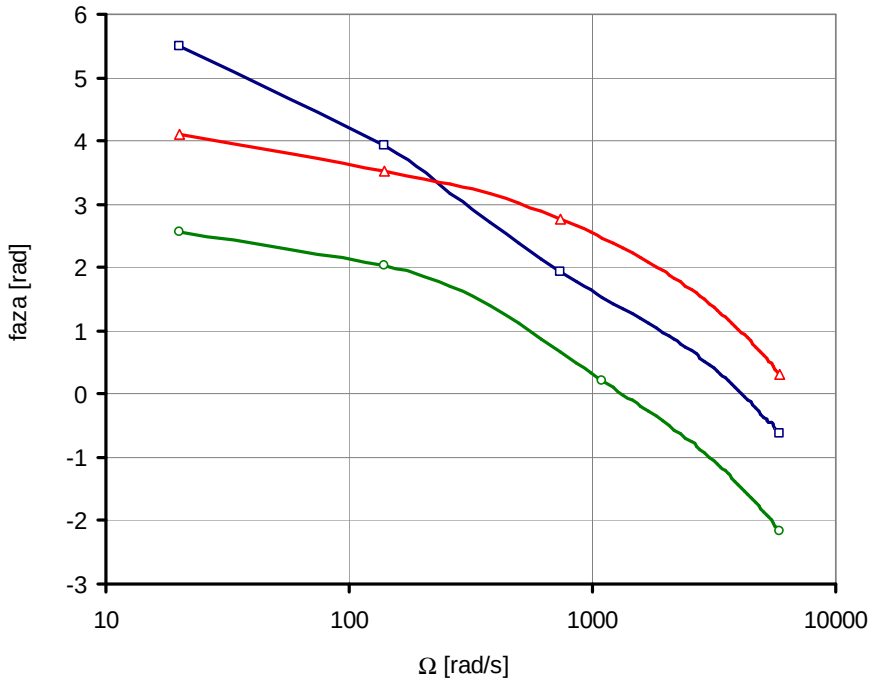

1–deflecion, 2 –phase change, 3 – total

- $a \ll \lambda_g$ (Ω < 460 rad/s $\Rightarrow \lambda_g$ = 1853 μm) $\Rightarrow$ BDS signal is phasial one,
- $a \sim \lambda_g \Rightarrow$ deflection component is the dominant one $\Rightarrow$ BDS signal increases with the increase in Ω *for* Ω > 2200 rad/s (λ_g < 847 μm).

Experiment

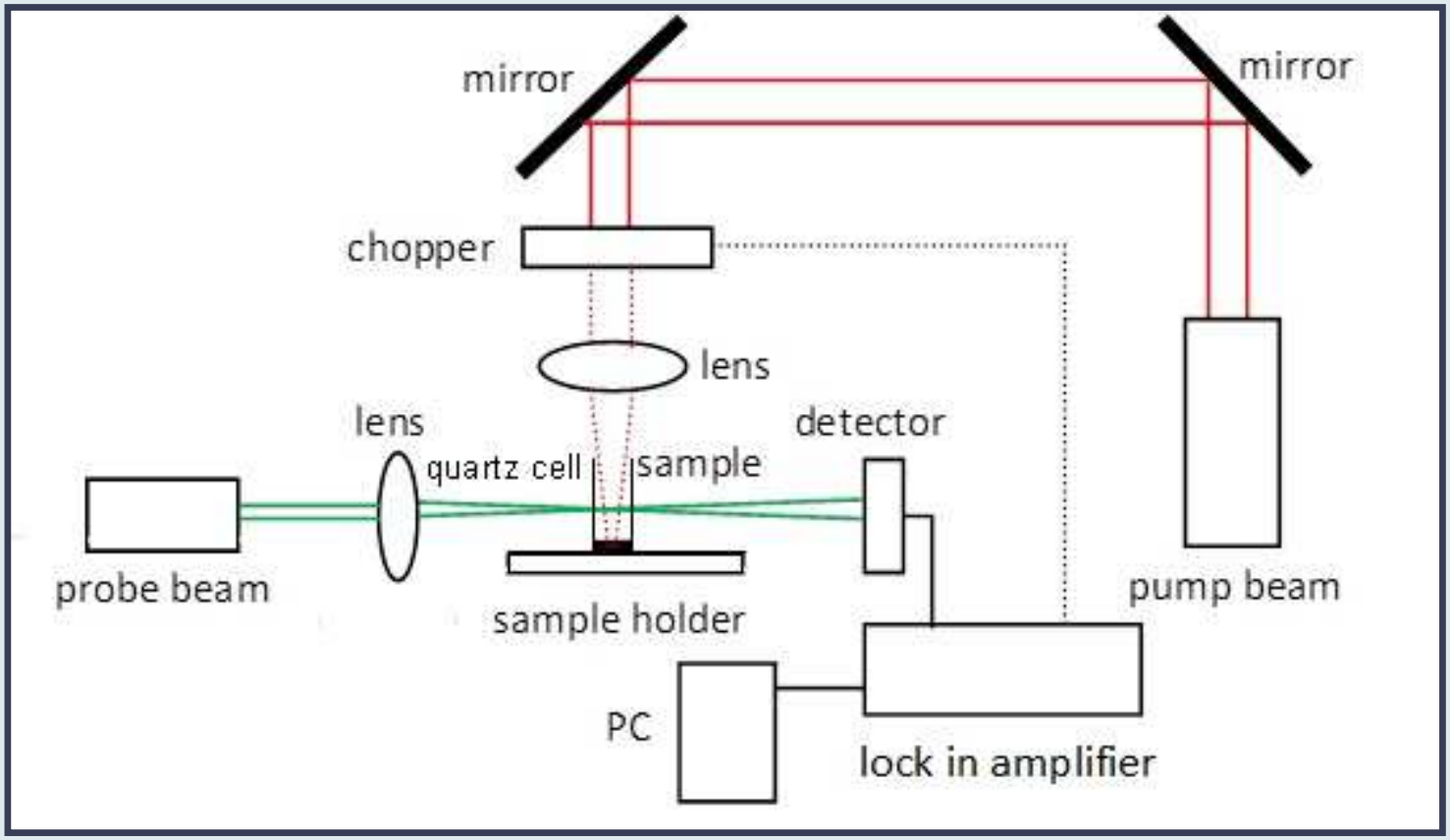
mirror
mirror
chopper
lens
lens
detector
quartz cell
sample
probe beam
sample holder
pump beam
PC
lock in amplifier

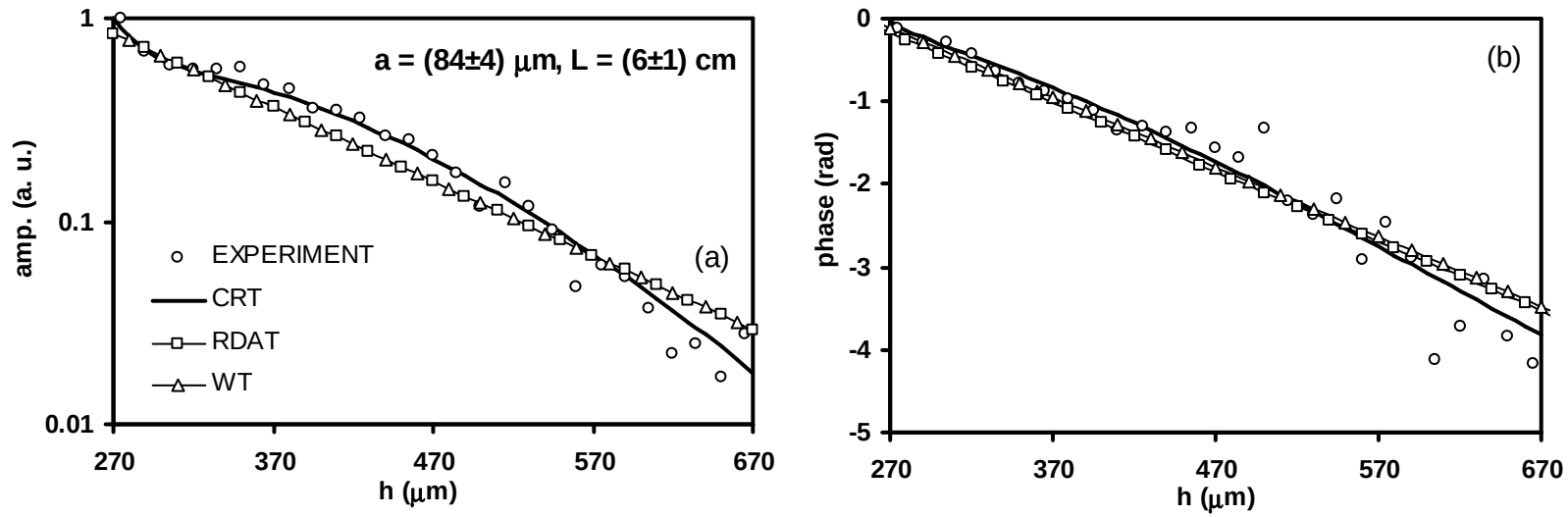

$a(z_l)$ = 215 μm, Ω = 3391 rad/s (λ_g = 682 μm)

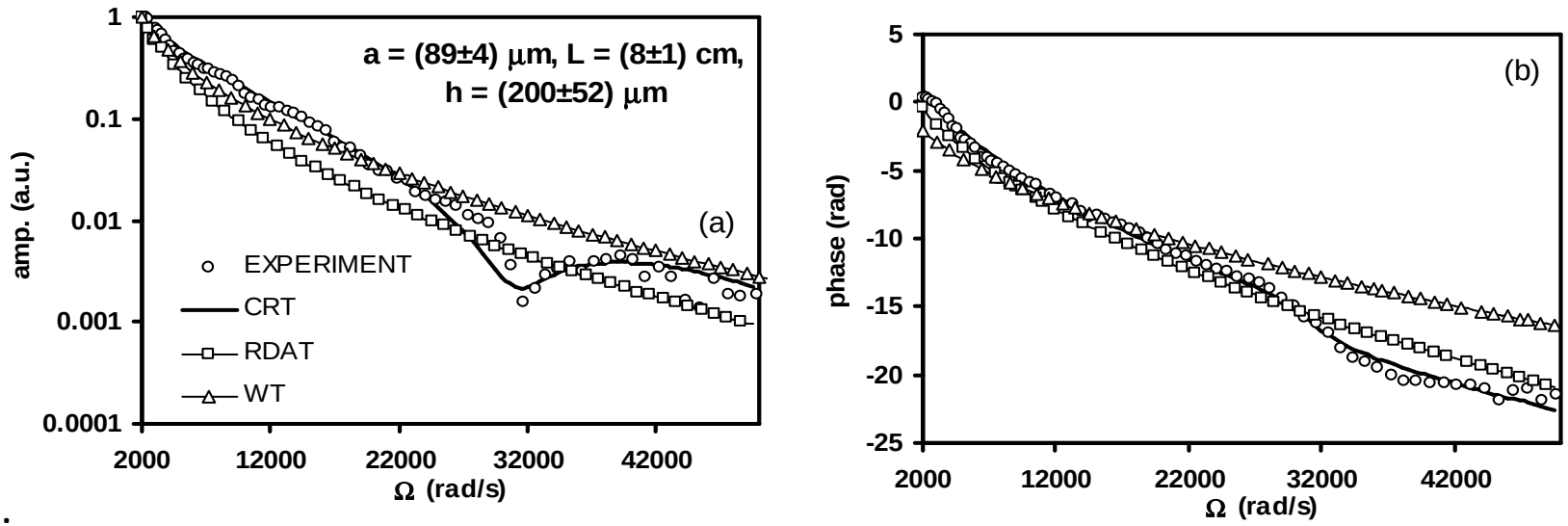

Table 1. Results of the sample thermal parameters and experimental setup parameters determination.

Material and tabulated thermal parameters	method	model	Values of determined parameters				
			κ (m^2/s)	k (W/mK)	a (μm)	L (cm)	h (μm)
zinc (κ = 4.18·10^{-5} m^2/s, k = 116 W/mK)[15]	$g(\Omega)$	CRT	4.42·10^{-5}	113	109	7.8	250
		WT	2.62·10^{-5}	56	109	7.3	250
		RDAT	2.38·10^{-5}	44	122	8.5	250
carbon (κ = 6.67·10^{-8} m^2/s, k = 0.081 W/mK)[15]	$g(h)$	CRT	6.58·10^{-8}	0.084	145	6.9	–
		WT	5.27·10^{-8}	0.062	156	6.2	–
		RDAT	5.15·10^{-8}	0.065	154	6.3	–

Using WT and RDAT may leads to errors especially in the case of measurements:

- when high modulation frequencies of temperature field are needed (eg. when thin samples or films are examined) ,
- large probe beam radius radius (a is comparable to the length of thermal wave λ_g) is required (eg. large samples).

Effect of sample's surface texture

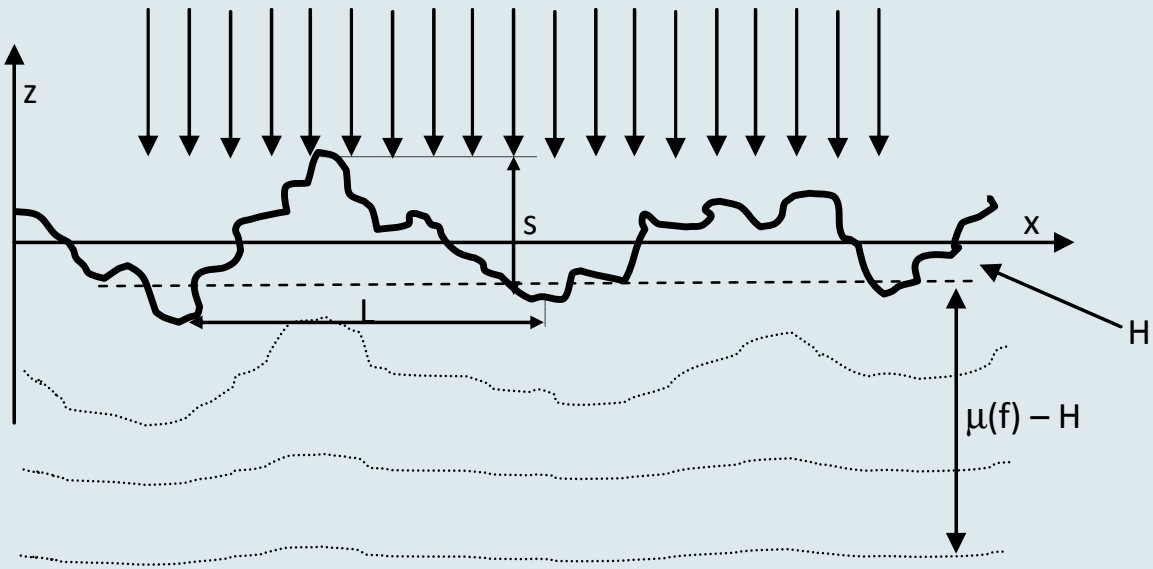

Surface roughness distorts the thermal wave's wave fronts leading to shortening its thermal diffusion length in the material, compared to a smooth surface μ, and consequently to decreasing thermal diffusivity and conductivity of the material.

shortened the thermal diffusion length: $\mu'(f) = \mu(f)[1 - H/\mu(f)]$

thermal diffusivity and conductivity: $\kappa_s'(f) = \kappa_s[1 - H/\mu(f)]^2 \quad k_s'(f) = k_s[1 - H/\mu(f)]^3$

Offset H depends on the surface profile $H(f) = \pi[Z(2\varsigma)/Z(2\varsigma+1)](s^2/L)$

s is the amplitude of surface roughness, L its periodicity , Z is Riemann's zeta function

Effect of particles introduction to the composite on material porosity

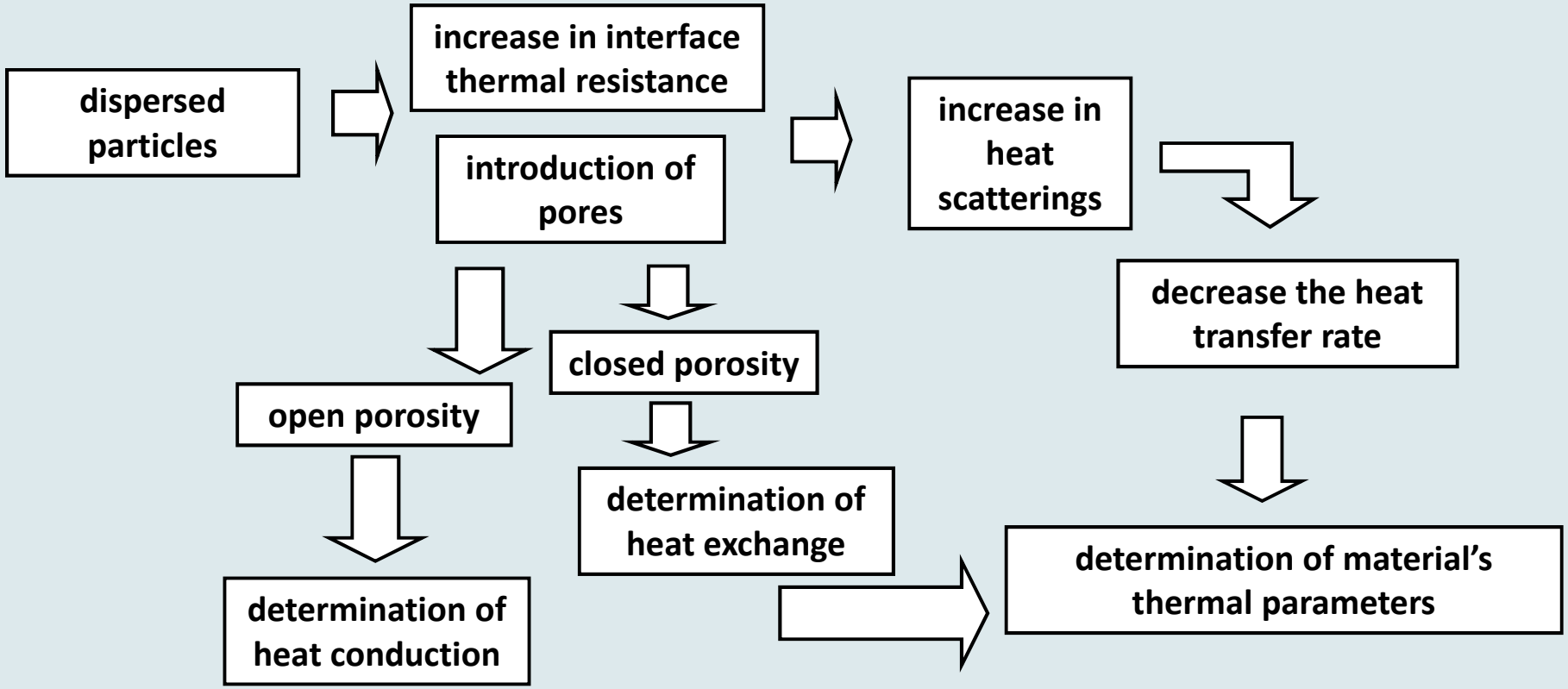

The material porosity determines the heat conduction in the material as well as its ability to heat exchange and reach the thermal equilibrium. $\Rightarrow$ define the values of sample's thermal parameters:

$$k = k_0 \frac{(\gamma+2)+2(\gamma-1)p}{(\gamma+2)-(\gamma-1)p} \qquad \kappa = \kappa_0 \frac{(\gamma+2)+2(\gamma-1)p}{(1+p)[(\gamma+2)-(\gamma-1)p]}$$

where γ is the ratio of thermal conductivity of cavities to that of the material,

p is the material's porosity,

k, κ is the thermal conductivity and diffusivity of porous material,

k_0, κ_0 is the thermal conductivity and diffusivity of material without cavities

SAMPLES

2 μm thick, pure TiO_2 and SiO_2/TiO_2 complex in a form of thin films deposited on Al support of 2 mm thickness

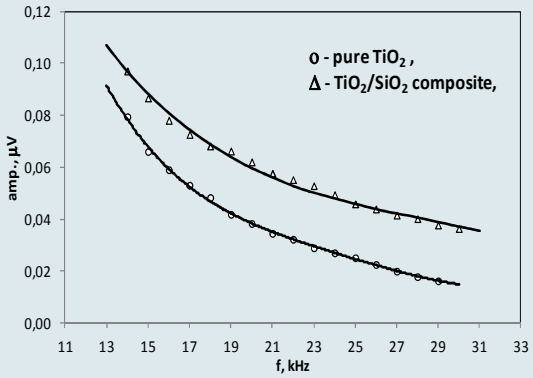

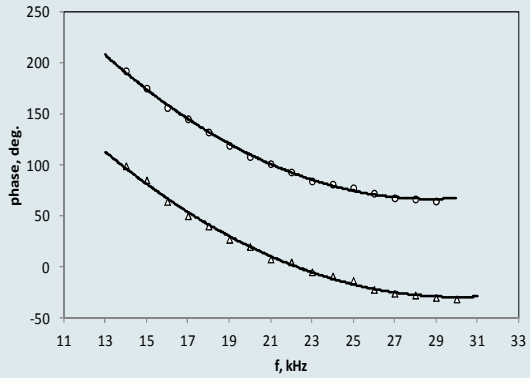

sample	BDS				
	10^{-6} κ_s, m^2s^{-1}	k_s, $Wm^{-1}K^{-1}$	s, μm	L, μm	porosity, %
TiO_2	1.40±0.05	2.50±0.05	2,40±0.05	3.50±0.10	12.8±0.6
TiO_2/SiO_2	1.25±0.10	2.30±0.10	1,40±0.05	5,35±0.20	6.0±0.5

AFM

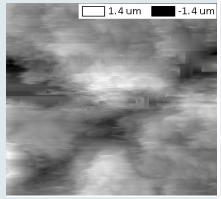

TIO_2	
s, μm	2.16±0.21
L, μm	5.27±1.30

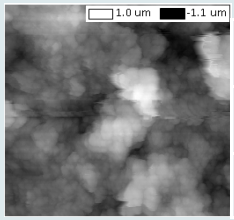

TiO_2/SiO_2	
s, mm	1.16±0.26
L, mm	6.01±0.45

porosity, %	
TiO_2	16.4±1.2
TiO_2/SiO_2	7.8±1.3

TiO_2/SiO_2 sample is less porous and less rough comparing to pure TiO_2 what is also expressed in the values of their thermal parameters

SAMPLES

ε-Fe_2O_3 based nanomaterials

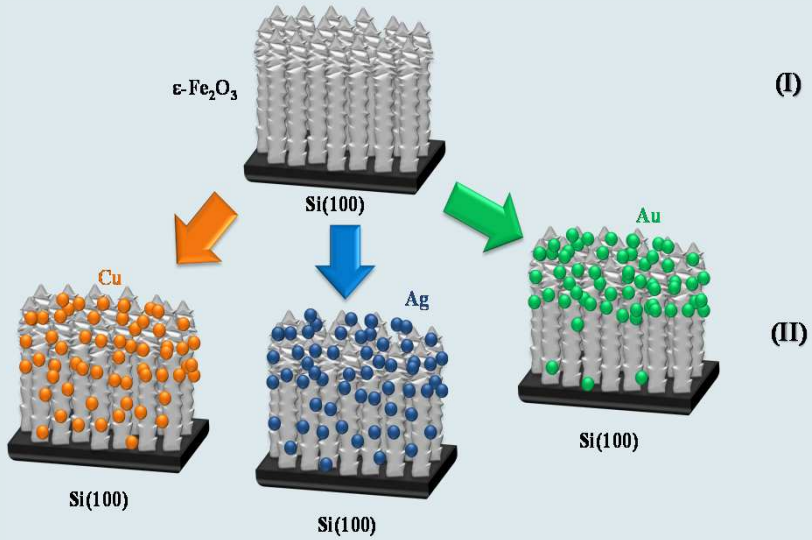

the power density of internal heat sources $q_i(z,t)$:

- Bulk recombination:

$$q_{BR}(z,t) = E_g n(z,t) t_{cr}^{-1}$$

E_g is the energy band gap, t_{cr} the carrier life time, $n(z,t)$ the density of photogenerated carriers,

- Surface recombination:

$$q_{SR}(z,t) = E_g \left[v_{SR0}\delta(z) + v_{SRl}\delta(z+l) \right] n(z,t)$$

v_{SR0} and v_{SRl} are surface recombination velocity at surface $z = 0$ and $z = -l$, respectively

- Intraband thermalization:

$$q_{IT}(z,t) = \alpha \frac{h\upsilon - E_g}{h\upsilon} I_0 \exp\left[\alpha(z+l) + i\Omega\, t\right]$$

That results from recombination of optically excited electron-hole pairs via phonon emission. α is the optical absorption coefficient of the sample

	ε-Fe_2O_3	Cu/ε-Fe_2O_3	Ag/ε-Fe_2O_3	Au/ε-Fe_2O_3
κ_s, cm^2s^{-1}	0.123±0.008	0.134±0.014	0.146±0.009	0.145±0.003
k_s, $Wm^{-1}K^{-1}$	14.5±0.7	26.0±1.2	20.0±1.4	21.0±1.2
E_g, eV	1.90±0.03	1.82±0.02	1.76±0.02	1.79±0.02
τ, ps	7.4±0.3	6.55±0.35	5.95±0.35	5.65±0.21

The NPs dispersed on ε-Fe_2O_3 nanomaterials act as an additional heat conducting channel improving thus the heat spreading ability of ε-Fe_2O_3.

The loading of Cu, Ag, or Au NPs on the ε-Fe_2O_3 matrices induced also a decrease in the band gap energy values along with an increase in the charge carrier transfer rate (eg. electrons to conductive band).

Investigation of frequency dependent photothermal beam deflection measurements in different thermooptical fluids

The experimental conditions can be optimized by placing the sample into ACN - a liquid with low thermal conductivity and high temperature coefficient of refractive index as compared to air.

SAMPLES

$CuFeInTe_3$ semiconductor

	-(dn/dT), 1/K	k, W/mK
Air	$3.7 \cdot 10^{-6}$	0.026
ACN	$4.5 \cdot 10^{+4}$	0.200

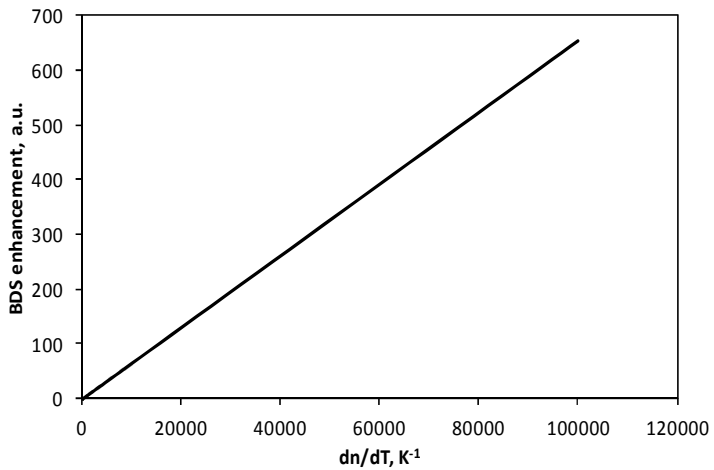

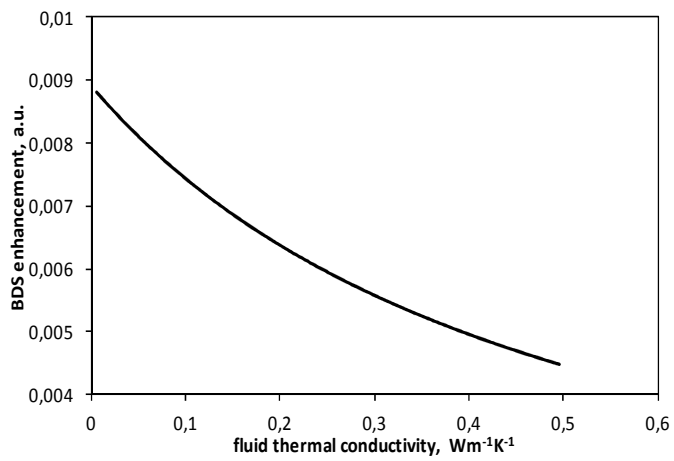

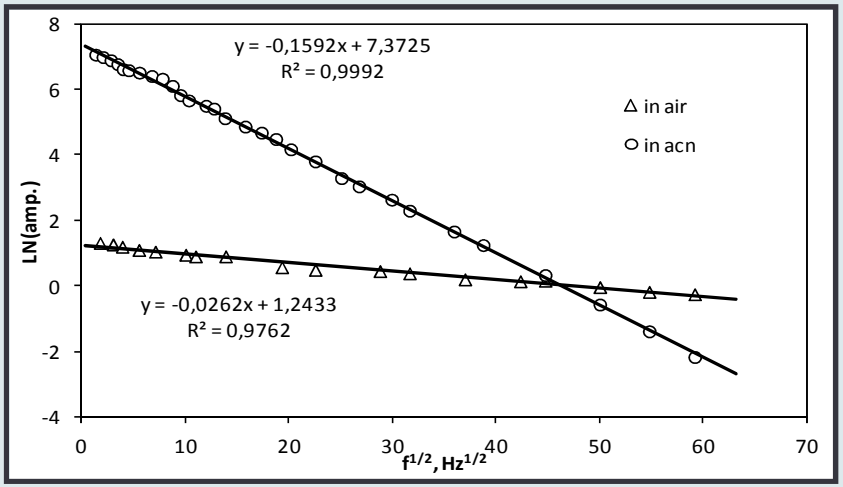

For sample immersed in ACN the registered BDS signal at lowest frequencies is up to 200 times higher compared to signals achieved in air.

These differences in signals' values decrease with increase in modulation frequency, reaching the same values for f = 2.3 kHz.

At higher frequencies the signal is higher in air.

	κ, m^2s^{-1}	k, $Wm^{-1}K^{-1}$
air	$(0.065\pm0.011)\times10^{-4}$	6.2 ± 0.8
ACN	$(0.052\pm0.005)\times10^{-4}$	5.8 ± 0.4

Since the BDS signal in ACN is much higher than in air for most of the used frequency range and the absolute measurement uncertainty is the same for all measuring points for both cases, the uncertainty of determined properties is better for the case of ACN.

Drug diffusion in multi layered structures

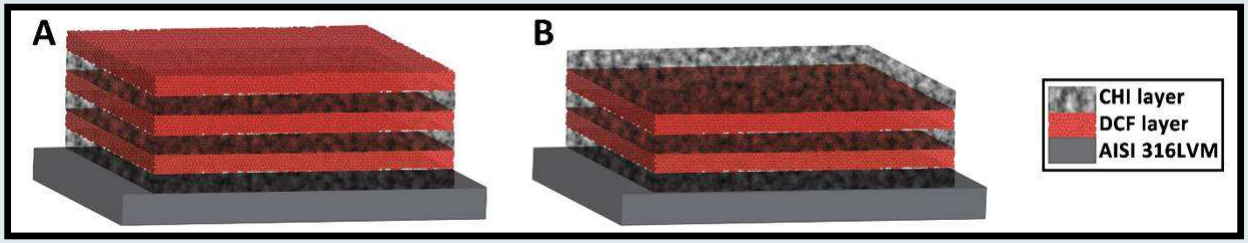

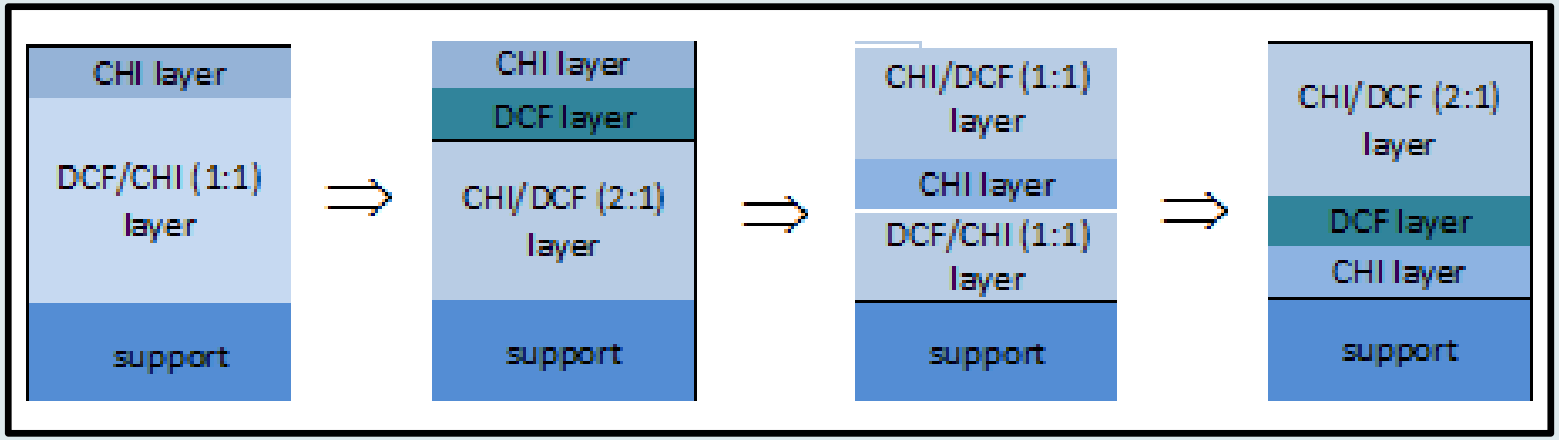

$$q_{si}(z,t)=\frac{\alpha_{si}I_0}{2}\exp\left[\sum_{m=1}^{j-1}\alpha_{sm}\left(l_{m-1}-l_m\right)+\alpha_{sj}\left(l_{j-1}-x\right)\right]\exp(i\Omega t)$$

DCF layer		
l_1, µm	κ. mm^2s^{-1}	k. $Wm^{-1}K^{-1}$
0.6	0.03	0.12

CHI layer		
l_1, µm	κ. mm^2s^{-1}	k. $Wm^{-1}K^{-1}$
0.7	0.18	0.20

CONCLUSIONS

1. BDS is a non-destructive and highly-sensitive technique, that requires minimum sample preparation,

2. It enables measurements of temperature increments on the sample surface at a level of 10^{-4} K, which correspond to a probe beam deviation angle of ~10^{-9} rad,

3. It enables detection absorption losses in solids at a level of ~10^{-7} cm^{-1},

4. It is applicable to measure optical (absorption coefficient), thermal (thermal conductivity, temperature), and electrical properties of materials that exhibit significant scattering (e.g. powders), optically thick or low absorbing samples that have no transmission.